Michigan State University

National Superconducting Cyclotron Laboratory

THE NSCL NEUTRON WALL FACILITY

P. ZECHER, A. GALONSKY, J. KRUSE, J. OTTARSON, J. WANG,
F. DEÁK, Á. HORVÁTH, Á. KISS, Z. SERES, AND K. IEKI

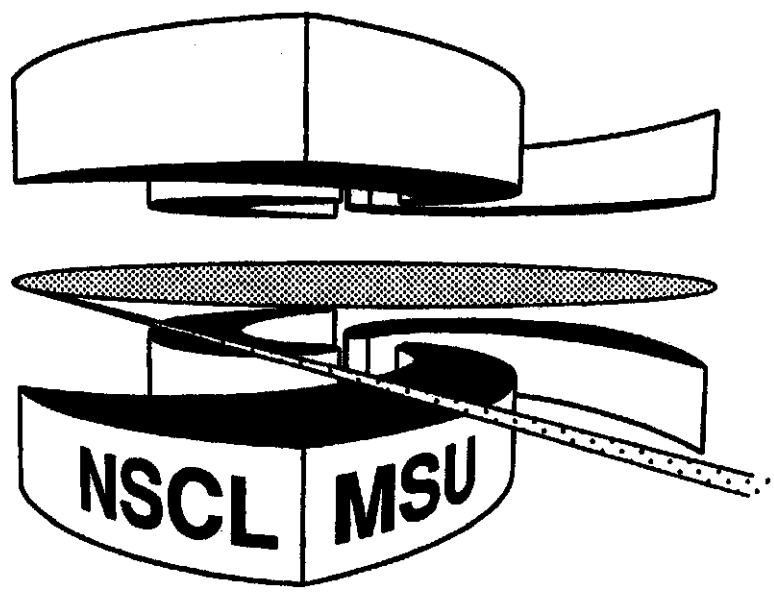

MSUCL-962

DECEMBER 1994

To be published in Proceedings of the
Workshop on Experimental Perspectives of Radioactive Nuclear Beam8
Padova, Italy, November 14-16, 1994

The NSCL Neutron Wall Facility

P. Zecher, A. Galonsky, J. Kruse, J. Ottarson, J. Wang
National Superconducting Cyclotron Laboratory,
Michigan State University, East Lansing, Michigan, USA

F. Deák, A. Horváth, A. Kiss
Department of Physics, Eötvös University,
Budapest, Hungary

z. seres
Central Research Institute for Physics
Budapest, Hungary

K. Ieki
Rikkyo University
Tokyo, Japan

We describe the design of the National Superconducting Cyclotron Laboratory's Neutron Wall detector, a large-area, high-efficiency, position-sensitive neutron detector.

Introduction

In early 1995, the National Superconducting Cyclotron Laboratory plans to commission a large-area, high-efficiency, position-sensitive neutron detector for use in radioactive nuclear beam experiments. We will describe the motivation behind the detector's design, the design criteria, how we plan on managing cross-talk and out-scattering, and the detector's final design.

Motivation

In 1991, an experiment to measure the soft-dipole-resonance parameters and ground state n-n correlations in ^{11}Li was performed at the NSCL [1,2]. To accomplish this, the complete kinematics of the reaction $^{11}\mathrm{Li} \rightarrow {}^{9}\mathrm{Li}$ + 2n were determined by measuring the position and energy of the reaction products. The experimental setup (shown in Figure 1) began with a 30 MeV/nucleon ^{11}Li beam produced by the A1200 fragment separator. The beam was incident on a Pb target after passing through two position-sensitive PPAC detectors used to determine the incident angle of the ^{11}Li. After dissociation in the Pb target, the ^{9}Li fragment's energy and position were measured in a Si/CsI telescope about 15 centimeters downstream from the target. The two neutrons passed through the telescope and were detected in two arrays consisting of 54 small scintillation detectors 5 and 6 meters downstream and subtending a half-angle of 5 degrees. Each neutron's energy was measured by its time-of-flight (TOF) and position by its detector's position.

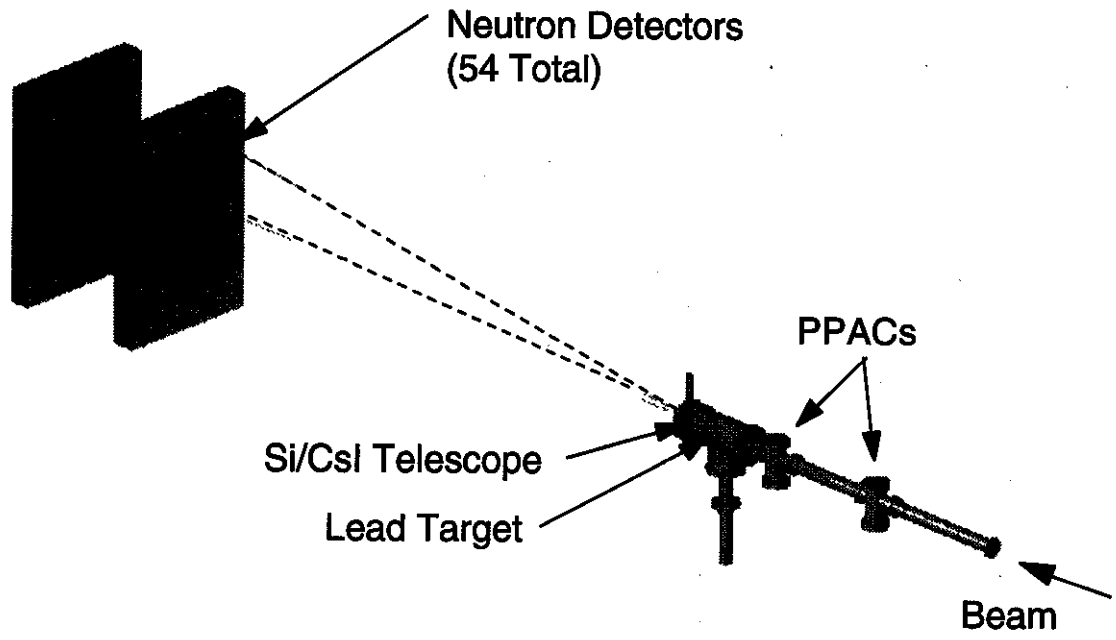

Figure 1 - Experimental setup for a previous experiment [1,2] performed at the NSCL to measure the total kinematics of the $^{11}Li \rightarrow ^{9}Li + 2n$ reaction.

Although the experiment was very successful, we would like to improve it and perform similar measurements on other neutron-rich halo-nuclei. One improvement we are making will reduce some of the limitations imposed by the array of small neutron detectors. Although the neutrons were forward focused, the acceptance angle of the array was small enough to reduce the solid angle efficiency for large break-up energies. The circular geometry of the individual detectors in the array creates an unavoidable 50 percent dead-space which also reduces the efficiency. This efficiency loss is even more acute because we need to detect two neutrons in coincidence. Even when a neutron enters the scintillator, the average detection efficiency is roughly 10 percent, so the efficiency for two neutron detection is 1 percent.

Having two thin arrays increases the efficiency without deteriorating the energy resolution. It is not possible to increase the thickness of the detectors to increase their efficiency without decreasing the energy resolution of the neutrons when using time-of-flight; the energy resolution is determined by the time resolution of the detector which is in-turn determined by its thickness. Unfortunately, adding the second array complicates the analysis by enhancing the effects of cross-talk and what we call out-scattering.

Cross-talk is the familiar problem of one neutron creating signals in two separate detectors; out-scattering is when a neutron scatters from the non-active part of a detector and is then detected in a different detector producing a distorted position and energy measurement. There are methods for identifying and eliminating cross-talk events from the data, but there are no methods for identifying out-scattering events. Therefore, the neutrons should pass through as little non-active material as possible. Unfortunately, the neutron detectors

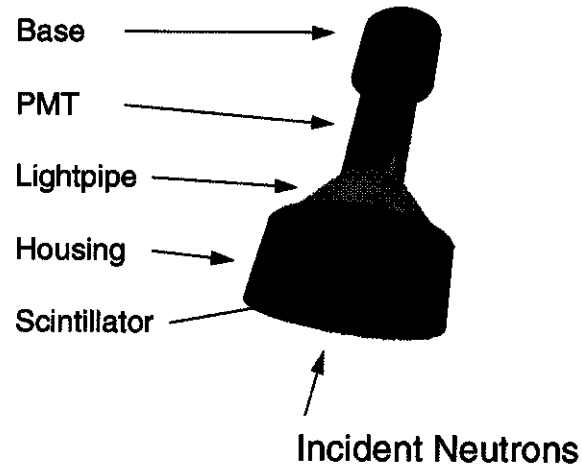

Figure 2 - A cut-a-way image of one of the neutron detectors used to make the neutron array for the ^{11}Li break-up experiment. The total mass of the detector was 4 kg and the mass of the scintillator was only 0.9 kg.

used in the array (see Figure 2) had a total mass to active mass ratio of over 4 to 1.

The New Design

Considering these limitations, we had four main objectives when designing the detector to replace the arrays:

1. increase the angular acceptance,
2. greatly reduce the dead-space,
3. reduce the mass of the non-active parts of the detector to reduce scattering,
4. accomplish this while increasing the scintillator mass to photomultiplier tube ratio.

The last point is simply one of cost-savings; as an example, if we duplicated the existing detectors so we could cover the same solid angle as we intend to cover with the new detector, we would need over 500 individual detectors with 500 channels of associated electronics.

To meet our objectives, we are using the well known geometry of long rectangular bars of scintillator, placed perpendicular to the beam axis, viewed at both ends by photomultiplier tubes (PMTs). By using 25 bars or cells of scintillator, each 2 meters long, we will cover an area of 4 m^2. Using the same flight path as in the previous experiment, the array will subtend a half-angle of 15 degrees where the previous array only subtend a half-angle of 5 degrees. A time signal for the TOF measurement is obtained from the mean time of time signals from the PMTs at the ends of a cell. The position of the event along the cell is determined from the time difference between signals. The thickness of the cell in the beam direction is determined by the energy resolution we wish to achieve with the 5 m flight-path. To increase the efficiency, we again place an identical array of 25 cells behind the first.

Complicating the design of the detector is a requirement that the detector be capable of pulse-shape-discrimination (PSD) to distinguish between neutron and γ-ray events. When the time-of-flight method is used to determine energy, a time-independent γ-ray background will introduce a constant background to the neutron spectrum; because we wish to study a continuous neutron spectrum, we must have some method of eliminating the γ-ray background from the neutron spectrum. The energy of the neutrons we wish to study is low enough that we will not be able to eliminate the γ-rays by setting a signal threshold above nuclear γ-ray energies. Also, γ-ray identification plays an important role in

cross-talk rejection. The complication in the design arises because the only scintillators capable of PSD are certain liquid hydrocarbon scintillators. Instead of the self-supporting plastic bars of scintillator which are usually employed in this configuration, our scintillator (NE-213) is housed in long, cast Pyrex tubes that are sealed at each end. The outside of the Pyrex cell is sufficiently smooth to allow for total internal reflection within the cell. By using total internal reflection instead of mirrored reflection or specular reflection, we are able to maintain the integrity of the light signal and perform the necessary PSD. The Pyrex cell does add to the non-active material that neutrons can interact with, but the proportion of total-mass to active-mass is much less than with our previous detector configuration.

To obtain the pulse shape discrimination, we exploit the different decay-time properties for signals from different charged particle species [3]. The charged particles we are most concerned with are electrons from γ-ray scattering and protons from elastic scattering with neutrons. To differentiate between the signals, we compare the signal's total charge to the charge in the signal's tail. (The tail is usually defined as beginning 30 ns after the start of the signal.) If we plot the total charge verses the tail charge, we obtain a 2D spectrum as shown in Figure 3, where the upper band represents the neutrons and the lower band the γ-rays.

When designing a detector which does PSD, it is useful to have a quantitative measure of the PSD so that different methods can be tested. The

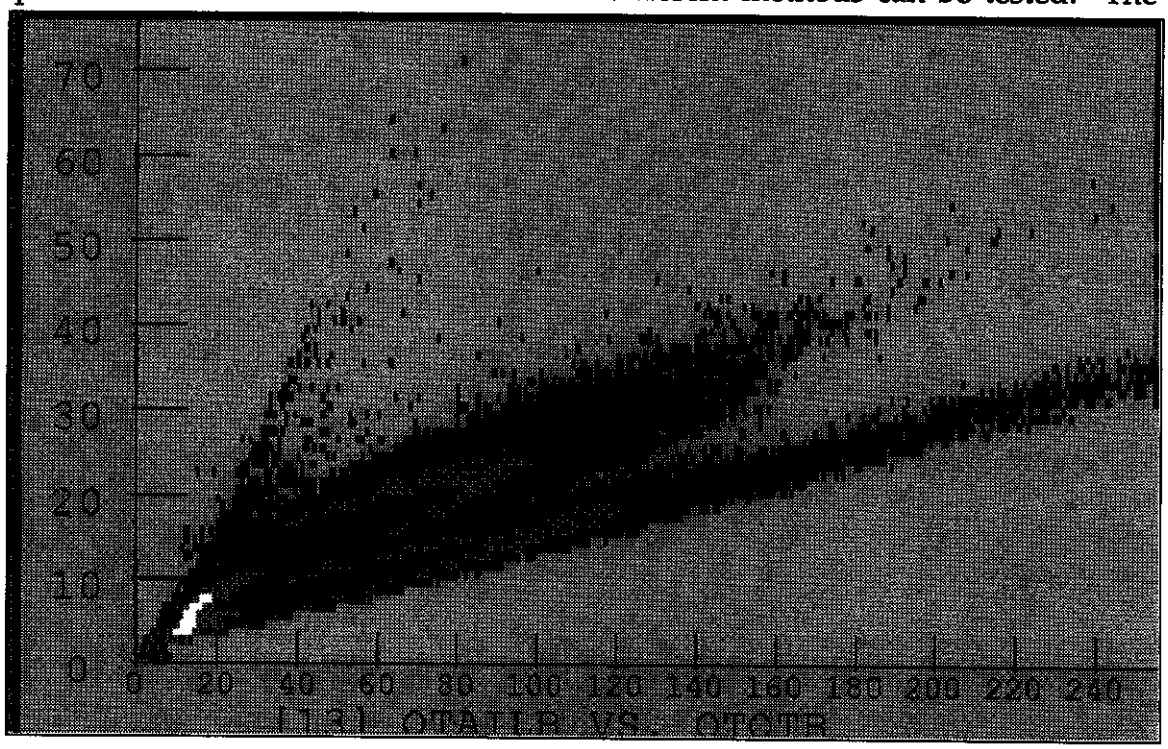

Figure 3 - A 2D spectrum showing the total integrated charge of the signal plotted along the abscissa verses the integrated charge of the signal's tail plotted along the ordinate.

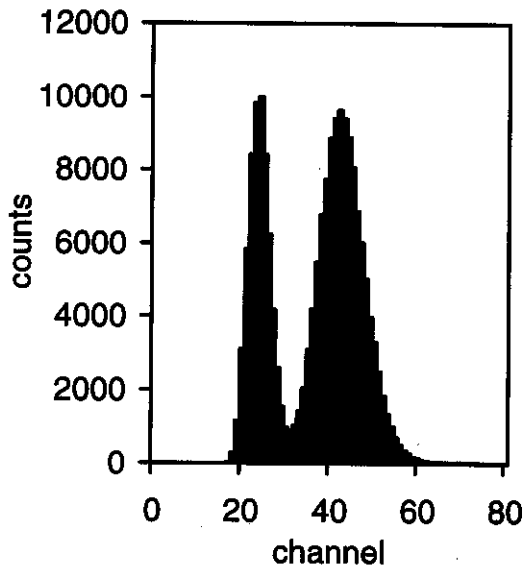

Figure 4 - A slice at a constant total charge from Figure 3. The first peak represents the γ-ray events and the second represents the neutron events. The total charge is equivalent to a 1.5 MeV electron.

standard number for evaluating n-γ PSD is the so-called Figure-Of-Merit (FOM). The FOM is defined for a fixed total charge; if we slice the data in Figure 3 at some constant total charge, we obtain a spectrum such as in Figure 4. In this spectrum, the first, narrow peak represents the γ-rays and the second, wider peak represents the neutrons. The FOM is then defined as the separation between the two centroids of the peaks divided by the sum of the FWHMs of the two peaks. We consider a FOM of 0.8 or above acceptable. The data in Figure 4 are from n-γ events at the center of a 2 meter cell and with a pulse-height corresponding to an electron energy of 1.5 MeV; the FOM is 1.07.

Cross-talk and Out-scattering

As mentioned earlier, placing a second array behind the first increases the problems of cross-talk and out-scattering. To explain how we attempt to manage these effects, it is useful to look at the main interactions that we can expect between the neutrons and the scintillator material. The scintillator is almost entirely hydrogen and carbon, and Table 1 lists the most likely interactions for neutrons in the scintillator. The first two have the largest cross-sections.

The (n,p) elastic scattering is our primary source of cross-talk. Figure 5 shows a typical example of a cross-talk event. In this case a single neutron scatters from a proton in the first wall, making a signal. The neutron does not lose all of its energy and proceeds to the second wall where it again scatters from a proton and makes another signal. To eliminate these events, we subject each two-pulse event to tests. If an event passes all three tests, it may be a cross-talk event. The three filters are:

1. The light pulse from the first scattered proton implies the proton's energy E_{P1}. From simple kinematics, E_{P1} implies

Table 1 - Listing of the predominant interactions for a neutron in the scintillator NE-213.

n + p → n + p
n + C → n + C
n + C → n' + C - 4.44 MeV
n + C → He + Be - 5.71 MeV
n + C → n' + 3He - 7.26 MeV
n + C → p + B - 12.59 MeV

the energy $E_{n'}$ of the scattered neutron and thus the scattering angle θ. If the scattering angle does not correspond to the location of the second pulse, then the event is not cross-talk.

2. If the scattered neutron's energy $E_{n'}$, as implied by E_{P1}, does not correspond with the energy as implied by the time-of-flight between the two walls, then the event is not cross-talk.
3. If the second scattered proton's energy E_{P2} is greater than the scattered neutron's energy $E_{n'}$, then the event is not cross-talk.

If the first recoil proton P1 does not have sufficient energy to be detected, then the event is no longer considered cross-talk and is considered out-scattering.

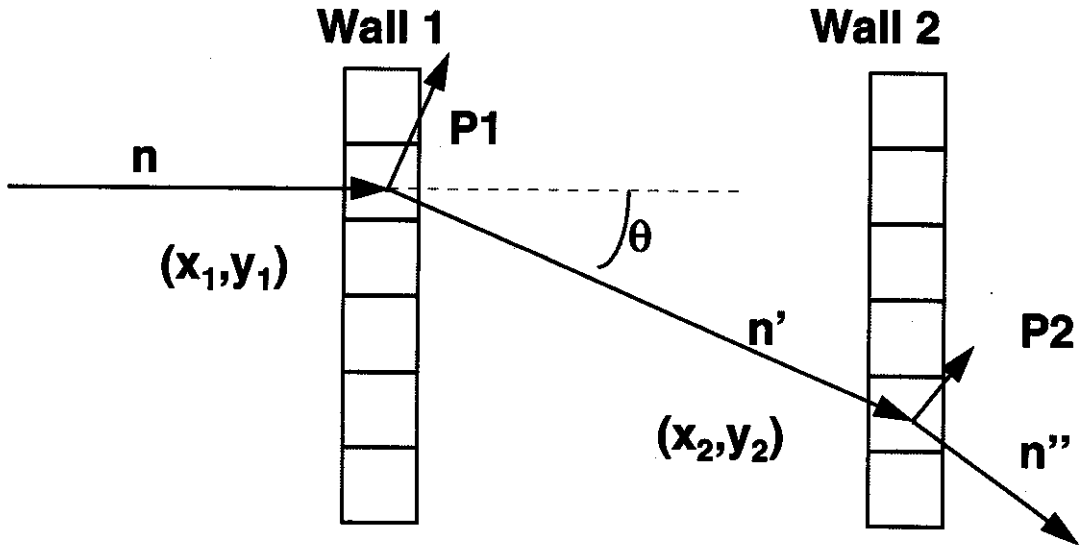

Figure 5 - A typical example of a cross-talk event.

Although most of the recoil protons will be detected, the recoil carbons will be too highly ionizing to ever produce enough light for detection [4]. (As an example, a 40-MeV carbon produces less light than a 1-MeV electron.) Therefore, the carbon in the scintillator effectively becomes non-active material and contributes to out-scattering. There is no way to identify these events, so we must rely on computer modeling to understand the effects. The majority of the out-scattering problem results in a loss of energy and position resolution in the second wall; the results of a Monte Carlo simulation of two-neutron detection is shown in Figure 6. This simulation assumed one neutron was detected in the first detector wall and the second neutron in the back detector wall; each neutron had an energy of 25 MeV, and the two neutrons had a relative momentum difference of 10 MeV/c. Figure 6 compares the effects on the relative momentum measurements caused by the position resolution, the cells' height, and the out-scattering. Although the effects of out-scattering are significant, they are comparable to other intrinsic resolution effects in the detector and thus we feel they are manageable. Our work on understanding the out-scattering and cross-talk effects is a continuing effort.

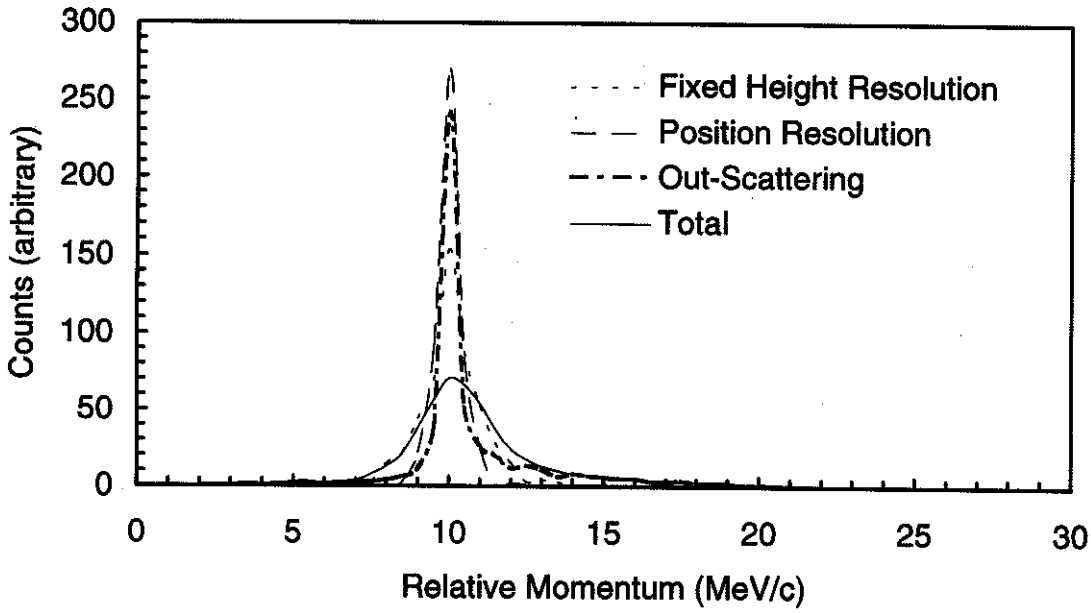

Figure 6 - The results of a Monte Carlo simulation that models the effects on relative momentum resolution caused by position resolution and out-scattering. The simulation assumed two neutrons, each with an energy of 25 MeV, and a relative momentum difference of 10 MeV/c. The *fixed height* curve represents the uncertainty introduced because of the height of the cell and the *position resolution* curve represents the uncertainty of the position measurement along the length of the cell.

The Final Design

The final design of the detector consists of two walls, each 2 meters by 2 meters in area, each containing 25 cells. There will be 10 liters of scintillator per cell. The cells have a cross-sectional area of 7.62 cm by 6.35 cm. An artist's conception of one of the walls, without the protective outer covering, is shown in Figure 7; one of the authors is shown standing next to the wall for scale. Figure 8 shows the position and time resolution we achieve with one of the cells; the data shown are measured by illuminating the center of the cell with a collimated γ-ray beam; the energy of the recoiling Compton electron is plotted along the x-axis.

Figure 9 shows early data for the FOM obtained from one of the cells. Each data set represents the FOM, as a function of energy, for a particular location along the cell as measured from the PMT. For the 2 meter cells, we are only concerned with the FOM for positions between a PMT and the center of the cell; as can be seen, we have achieved our desired 0.8 FOM for those positions. The energy scale is measured in MeVs of electron-equivalent energy. More recent data show an improvement in the FOM, such that the FOM measured at the center of the cell is above 1.0 for energies above 1.0 MeVee.

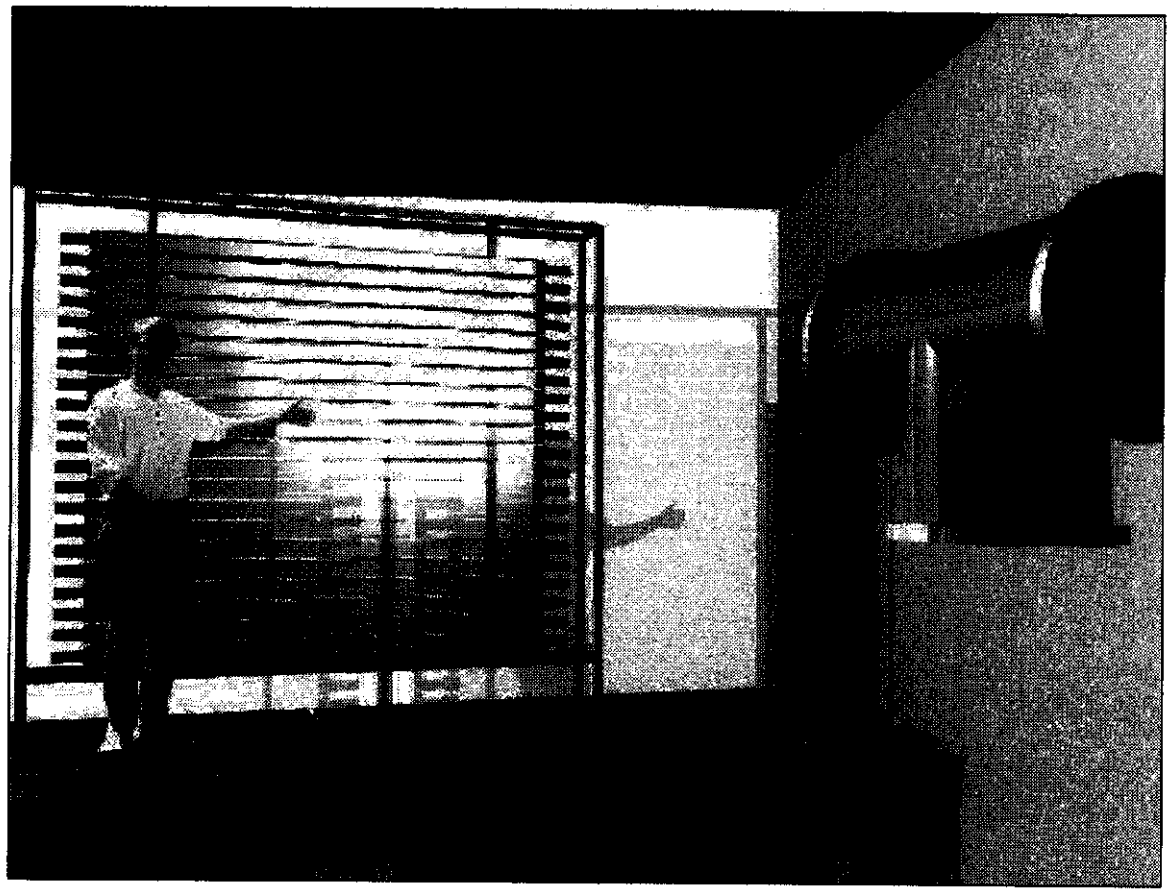

Figure 7 - An artist's conception of one of the Neutron Walls, without the protective outer covering. One of the authors is shown for scale; he is approximately 185 cm tall.

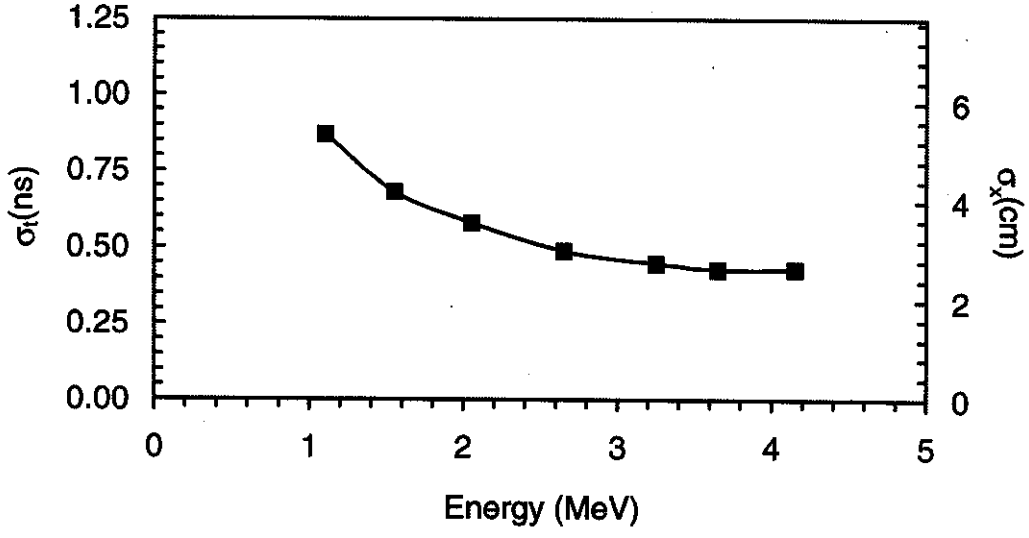

Figure 8 - The time and position resolution of a 2m cell, measured at the center of the cell. The measurements were made with a collimated γ-ray source.

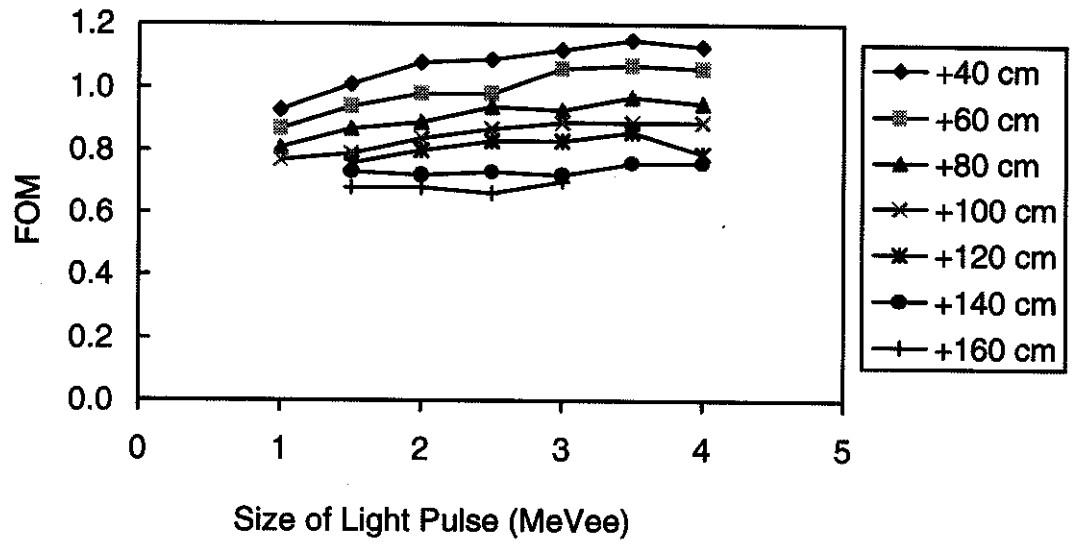

Figure 9 - The FOM for various positions along the length of a cell as measured from the PMT. The data are plotted against the light-output of the pulse, measured in units of electron-equivalent energy.

The Neutron Walls are in their final stages of construction and we plan on commissioning them in early 1995. Before we perform any of the 2-neutron coincidence experiments, single-neutron experiments will be performed to measure the effects of cross-talk and out-scattering so we will have empirical data to compare to our computer models.

Acknowledgments

We wish to gratefully acknowledge the support of the US National Science Foundation under Grant Numbers INT91-13997 and PHY92-14992 and the Hungarian Academy of Sciences.

References

1. D. Sackett et al., Phys. Rev. C **48**, 118 (1993)
2. K. Ieki et al., Phys. Rev. Lett. **70**, 730 (1993)
3. J.H. Heltsley et al., Nucl. Instrum. Methods **A263**, 441 (1988)
4. V.V. Verbinski, et al., Nucl. Instrum. Methods **65**, 8 (1968)